

An Efficient Construction Method Based on Partial Distance of Polar Codes with Reed-Solomon Kernel

Jianhan Zhao, Wei Zhang, Yanyan Liu

Abstract—Polar codes with Reed-Solomon (RS) kernel have great potential in next-generation communication systems due to their high polarization rate. In this paper, we study the polarization characteristics of RS polar codes and propose two types of partial orders (POs) for the synthesized channels, which are supported by validity proofs. By combining these partial orders, a Partial Distance-based Polarization Weight (PDPW) construction method is presented. The proposed method achieves comparable performance to Monte-Carlo simulations while requiring lower complexity. Additionally, a Minimum Polarization Weight Puncturing (MPWP) scheme for rate-matching is proposed to enhance its practical applicability in communication systems. Simulation results demonstrate that the RS polar codes based on the proposed PDPW construction outperform the 3rd Generation Partnership Project (3GPP) NR polar codes in terms of standard code performance and rate-matching performance.

Index Terms—5G, polar codes, Reed-Solomon codes, rate-matching, partial order

I. INTRODUCTION

POLAR codes presented by Arikan [1] were proved to achieve the capacity of binary-input symmetric discrete memoryless channels (BI-DMC). In a polar code with block length N and rate of R , the key process is to select NR sub-channels with high reliability to directly transmit information, thereby approximating the channel capacity. To decode polar codes, successive cancellation (SC) decoders were initially used, which have a time complexity of $\mathcal{O}(N \log N)$.

However, as the incomplete channel polarization in the finite regime, the performance of polar codes with short or moderate block lengths is not ideal. Therefore, researchers have focused on improving polar codes performance by developing decoding algorithms and construction methods. In terms of decoding algorithms, the successive cancellation list (SCL) [2]–[4] decoding and the successive cancellation stack (SCS) [5]–[7] decoding have been proposed and improved, which achieve a good decoding performance. Concatenating with a Cyclic Redundancy Check (CRC) code further improves the performance. In terms of construction methods, several algorithms have been proposed, such as Tal-Vardy method [8] and Gaussian approximation (GA) [9]. Practical communication systems such as the 5G system require channel coding with flexible codewords to take full advantage of limited resources

and accommodate changeable code rates. To address this, Quasi-uniform puncturing (QUP) [10] and Information Set Approximation Puncturing (ISAP) [11] have been proposed, demonstrating good rate-matching performance. Due to these excellent performance characteristics, polar codes have been accepted as the coding scheme for the 5G new radio (5G NR) control channel [12].

Multi-kernel polar codes have recently gained attention in [13]–[18] due to their superior performance. Specifically, polar codes over $\mathcal{GF}(q)$ with Reed-Solomon (RS) kernel can achieve a higher polarization rate than the Arikan kernel [16], [19]. Several pioneering works have been conducted to design polar codes with RS kernel. Results in [16] demonstrate that the polar codes with 4-dimension RS kernel could already achieve a better performance than most binary kernels. Cheng *et al.* have proposed a look-up table-based encoding algorithm [20] for polar codes with RS kernel, which significantly reduces the encoding complexity. In [21], an effective decoding scheme using “dynamic frozen symbols” is proposed to improve decoding performance. Furthermore, [22] presents a piecewise sequence rate-matching scheme to achieve flexible code rates.

However, few studies have investigated the construction of polar codes with RS kernel. Most previous studies, as mentioned above, have relied on Monte-Carlo simulations, which are not efficient and are difficult to apply to practical communication systems. In recent studies, partial orders (POs) were shown to exist between the reliabilities of the sub-channels of polar codes with Arikan kernel [23]–[25]. Based on these partial orders, construction methods with low complexity were proposed in [26], [27]. These works enlighten us to pursue an efficient construction scheme of polar codes with RS kernel for practical transmission channels.

In this paper, we focus on studying the polarization characteristics of polar codes with RS kernel, especially the relationship between the sub-channel index and its channel reliability. We first present partial orders for polar codes with RS kernel that are independent of the underlying channel W . These POs are based on the observation of the relationship between the reliability of symbol sub-channels and the q -ary representation of their channel indexes. Combining the POs results, we propose a Partial Distance-based Polarization Weight (PDPW) construction method with lower complexity, while ensuring performance guarantees. Finally, based on the polarization weight, an efficient rate-matching scheme of polar codes with RS kernel is proposed which can be applied to more flexible communication systems.

The remainder of the paper is organized as follows. In Section II we provide a brief overview of polar codes and the

Jianhan Zhao, Wei Zhang are with the School of Microelectronics, Tianjin University, Tianjin 300072, China (e-mail: zjh1997@tju.edu.cn; tjuzhangwei@tju.edu.cn).

Yanyan Liu is with the Tianjin Key Laboratory of Photoelectronic Thin Film Devices and Technology, Nankai University, Tianjin 300071, China (e-mail: lytianjin@nankai.edu.cn).

Digital Object Identifier —

Reed-Solomon (RS) kernel. Section III proposes two partial orders for the polarization properties of polar codes with RS kernel and describes the proposed PDPW construction method. In Section IV, a Minimum Polarization Weight Puncturing (MPWP) scheme is presented to evaluate the rate-matching performance. Then, in Section V, the simulation results of the proposed algorithms are presented. Finally, Section VI concludes this work.

II. PRELIMINARIES

A. Notations and Channel Parameters

Throughout the paper, n , t and m is non-negative integers. Let N and N_b denote the symbol length and bit length of a code, respectively. Denote u_0^{N-1} as the row vector $\{u_0, u_1, \dots, u_{N-1}\}$.

Definition 1. Let \mathcal{X} and \mathcal{Y} be the q -ary input alphabet and output alphabet for a channel $W : \mathcal{X} \rightarrow \mathcal{Y}$. We define the mutual information of channel W as follows:

$$I(W) = \sum_{x \in \mathcal{X}} \sum_{y \in \mathcal{Y}} \frac{1}{q} W(y|x) \log \frac{W(y|x)}{\frac{1}{q} \sum_{x' \in \mathcal{X}} W(y|x')} \quad (1)$$

Definition 2. The Bhattacharyya parameter of a q -ary channel W is defined as

$$Z(W) = \frac{1}{q(q-1)} \sum_{x \in \mathcal{X}, x' \in \mathcal{X}, x \neq x'} Z_{x,x'}(W) \quad (2)$$

where for any input symbols $x, x' \in \mathcal{X}$ the Bhattacharyya parameter is defined as

$$Z_{x,x'}(W) = \sum_{y \in \mathcal{Y}} \sqrt{W(y|x)W(y|x')} \quad (3)$$

Definition 3. Let \mathcal{X} and \mathcal{Y} be the q -ary input alphabet and output alphabet for a channel $W : \mathcal{X} \rightarrow \mathcal{Y}$ with the basic input $x \in \mathcal{X}$ and $y \in \mathcal{Y}$. Denote the $\mathcal{D}_x = \{y \in \mathcal{Y} \mid W(y|x) > W(y|x'), \forall x' \in \mathcal{X}, x' \neq x\}$. The average error probability of the maximum-likelihood estimation of channel W is defined as :

$$P_e(W) = \frac{1}{q} \sum_{x \in \mathcal{X}} \sum_{y \in \mathcal{D}_x^c} W(y|x). \quad (4)$$

where $P_e(W)$ is bounded as

$$P_e(W) \leq (q-1)Z(W) \quad (5)$$

Definition 4. (Stochastic Degradation [8]): Let W_1, W_2, W_3 be the channels $\mathcal{X} \rightarrow \mathcal{Z}$, $\mathcal{X} \rightarrow \mathcal{Y}$ and $\mathcal{Y} \rightarrow \mathcal{Z}$, we say W_1 is stochastically degraded with respect to W_2 , denoted as $W_2 \succeq W_1$ if their relationship exist such that

$$W_1(z|x) = \sum_{y \in \mathcal{Y}} W_2(y|x)W_3(z|y) \quad (6)$$

Definition 5. (Reliability measure): For two synthetic channels $W_N^{(i)}$ and $W_N^{(j)}$, if $W_N^{(i)} \succeq W_N^{(j)}$ or $i \geq j$, we say $W_N^{(i)}$ is more reliable than $W_N^{(j)}$ then

$$I(W_N^{(i)}) \succeq I(W_N^{(j)}) \quad (7)$$

$$Z(W_N^{(i)}) \preceq Z(W_N^{(j)}) \quad (8)$$

$$P_e(W_N^{(i)}) \preceq P_e(W_N^{(j)}) \quad (9)$$

B. Arikan Polar Codes

For an Arakan polar code with length $N = 2^n$, the indices of the sub-channels $W_N^{(i)}$ after channel polarization can be expressed as $\{0, 1, \dots, N-1\}$. Let $\mathcal{I} \subseteq \{0, 1, \dots, N-1\}$ be the information-bit set that contains the indices of the K most reliable sub-channels carrying information bits. Its complement \mathcal{F} represents the frozen-bit set. The generator matrix is $F_N = G_2^{\otimes n}$, where kernel $G_2 \triangleq \begin{bmatrix} 1 & 0 \\ 1 & 1 \end{bmatrix}$ and \otimes denotes the Kronecker product of the matrix with itself. The block error performance of polar codes can be expressed as

$$P_B = o\left(2^{-N^\epsilon}\right), \quad \forall \epsilon < E(G) \quad (10)$$

where the threshold $E(G)$ of ϵ is the exponent of kernel G as introduced in [15]. For instance, the Arikan kernel G_2 has an exponent of 0.5, and kernels with larger exponents can achieve better performance.

C. Reed-Solomon Kernels

Reed-Solomon Kernels can be regarded as a generalization of Arikan kernel. In the case of a channel with input alphabet $\mathcal{GF}(q = 2^t)$, one can obtain the q -ary matrix G_q . The submatrix of G_q that consists of the i -th row to the $(q-1)$ -th row is a generator matrix of a generalized Reed-Solomon code. Therefore, we refer to the q -ary matrix G_q as the Reed-Solomon kernel, e.g.

$$G_q = \begin{pmatrix} 1 & 1 & \dots & 1 & 1 & 0 \\ \alpha_{q-2}^{q-2} & \alpha_{q-3}^{q-2} & \dots & \alpha_1^{q-2} & 1 & 0 \\ \vdots & \vdots & \ddots & \vdots & \vdots & \vdots \\ \alpha_{q-2}^1 & \alpha_{q-3}^1 & \dots & \alpha_1^1 & 1 & 0 \\ \alpha_{q-2}^0 & \alpha_{q-3}^0 & \dots & \alpha_1^0 & 1 & \gamma \end{pmatrix} \quad (11)$$

where α_i are primitive element of $\mathcal{GF}(q)$ and γ is a non-zero element of $\mathcal{GF}(q)$.

By analogy with the Arikan kernel, we can construct an RS polar code of symbol length $N = q^m, m \in \mathbb{Z}^+$ over $\mathcal{GF}(q)$. For a q -ary symbols information sequence s_0^{N-1} , its corresponding encoded codeword can be expressed as $c_0^{N-1} = s_0^{N-1}F_N = s_0^{N-1}G_q^{\otimes m}$. If symbol c_i are transmitted over a memoryless output-symmetric channel $W(y|c)$, then after channel polarization, the q -ary synthetic sub-channels with their respective transition probabilities can be defined as follow:

$$W_N^{(i)}(y_0^{N-1}, s_0^{i-1} | s_i) = \frac{1}{q^{N-1}} \sum_{s_{i+1}^{N-1}} \prod_{i=0}^{N-1} W(y_i | (s_0^{N-1}F_N)_i) \quad (12)$$

More specifically, let $(i_{m-1}, \dots, i_1, i_0)$ be the q -ary representation of the index i , i.e.,

$$i = \sum_{k=0}^{m-1} i_k q^k \quad (13)$$

Then, we define the $W_N^{(i)}$ as

$$W_N^{(i)} = \left(\left((W^{i_0})^{i_1} \right) \dots \right)^{i_{m-1}} \quad (14)$$

In addition, for polar codes with multi-kernel, the kernel exponent is represented as

$$E(G) = \ln(q!)/(q \ln q) \quad (15)$$

For instance, when $q = 2^2$, the exponent of the Reed Solomon kernel G_4 is $\ln 24/(4 \ln 4) \approx 0.57312$, which is larger than the exponents of most binary linear kernels in [15], despite its small and simple structure. Therefore, the RS kernel achieves a higher polarization rate, and its performance is better when constructing codewords of the same block length.

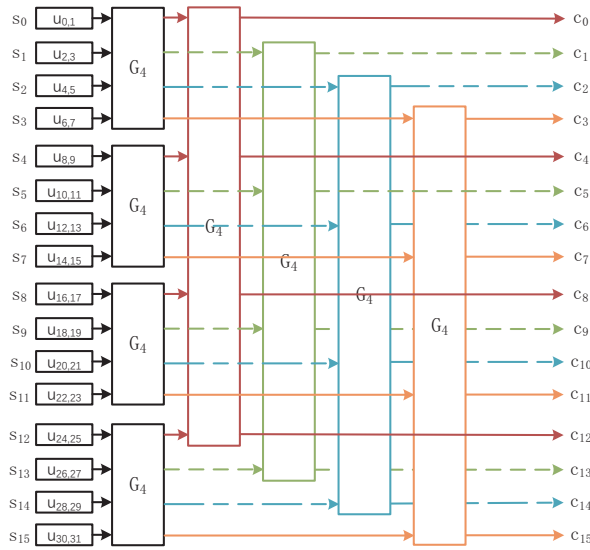


Fig. 1. Polar codes with RS kernel with $q = 4$ and $m = 2$.

In practice, taking G_4 kernel as an example,

$$G_4 = \begin{bmatrix} 1 & 1 & 1 & 0 \\ \alpha & \alpha^2 & 1 & 0 \\ \alpha^2 & \alpha & 1 & 0 \\ 1 & 1 & 1 & \alpha \end{bmatrix} \quad (16)$$

the scheme of RS polar codes with $q = 4$ and $m = 2$ using the G_4 kernel is illustrated in Fig. 1.

When constructing polar codes using the G_4 kernel, every two bits are mapped into a q -ary symbol over $\mathcal{GF}(q)$ as shown below:

$$(0, 0) \leftrightarrow 0, \quad (0, 1) \leftrightarrow \alpha, \quad (1, 0) \leftrightarrow \alpha^2, \quad (1, 1) \leftrightarrow \alpha^3. \quad (17)$$

Note that the mapping is not unique and the addition and multiplication are based on the $\mathcal{GF}(q)$ operations in [20].

D. Rate-matching Scheme

In practical communication system, flexible code length and rate are required. Therefore, the standard codeword needs to be adjusted utilizing rate-matching method before transmission to the channel. A typical rate-matching scheme for RS polar codes is illustrated in Fig.2. As mentioned in the previous subsection, the N size RS polar codes contain fixed q^m symbols ($N_b = t \times q^m$ bits). After a specific rate-matching algorithm, the actually transmitted code block length in bits is M_b , where $M_b < N_b$. Thus, the actual transmission block rate is defined as $R = K_b/M_b$. On the receiver side, the decoding

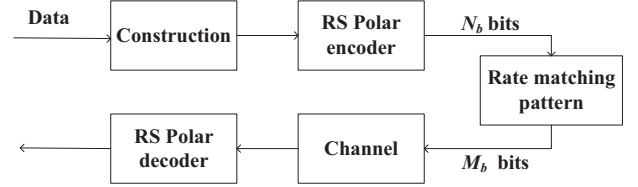


Fig. 2. Rate-matching scheme for polar codes with RS kernel

structure remains the same. Since the $N_b - M_b$ bits are not sent over the channel, their initial log-likelihood ratios (LLR) for the decoder are set to zero or infinity depending on different rate-matching algorithms.

III. AN EFFICIENT CONSTRUCTION OF POLAR CODES WITH REED-SOLOMON KERNEL

In this section, we first investigate the reliability relationship of sub-channels in a single-layer RS kernel. We then introduce the concept of partial orders (POs) for RS polar codes. Finally, we utilize these POs to propose an efficient construction method for polar codes with RS kernel.

A. Channel Degradation of Polar Codes with RS Kernel

Denote the subchannel $W_{G_q}^{(i)}$ for a $q \times q$ RS kernel G_q as

$$W_{G_q}^{(i)} \triangleq s_i \rightarrow (y_0^{q-1}, s_0^{i-1}) \quad (18)$$

and the transition probabilities as

$$W_{G_q}^{(i)}(y_0^{q-1}, s_0^{i-1} | s_i) = \frac{1}{q^{q-1}} \sum_{s_{i+1}^{q-1}} W_{G_q}(y_0^{q-1} | s_0^{q-1}) \quad (19)$$

where

$$W_{G_q}(y_0^{q-1} | s_0^{q-1}) \triangleq \prod_{i=0}^{q-1} W(y_i | c_i) = \prod_{i=0}^{q-1} W(y_i | (s_0^{q-1} G_q)_i) \quad (20)$$

As the RS kernel G_q is invertible, the following equation holds

$$\sum_{i=0}^{q-1} I(W_{G_q}^{(i)}) = qI(W) \quad (21)$$

Given a q -ary DMC $W : \{0, 1, \dots, q-1\} \rightarrow \mathcal{Y}$, denote the transition probabilities of channel $\tilde{W} : \{0, \dots, q-1\} \rightarrow \mathcal{Y} \times \{0, \dots, q-1\}$,

$$\tilde{W}(y, r | c) = \frac{1}{q} W(y | s + r) \quad (22)$$

Then, let $(W \otimes P)$ denote the channel with transition probabilities $(W \otimes P)(y_1, y_2 | c) = W(y_1 | c)P(y_2 | c)$ and the $W^{\otimes k}$ denote k operations on W itself.

$$W^{\otimes k}(y_1^k | c) = \prod_{j=1}^k W(y_j | c) \quad (23)$$

In addition, it is easy to prove that

$$(W^{\otimes k})^{\otimes h} = W^{\otimes kh} = \prod_{j=1}^{kh} W(y_j | c) \quad (24)$$

Since the RS kernel G_q is invertible and polarizing [16], for all q -ary DMCs W , there exists a channel $W_{G_q}^{(i)}$ which is statistically equivalent to either $\tilde{W}^{\otimes k}$ or $W \otimes \tilde{W}^{\otimes k-1}$, where $i \in \{0, 1, \dots, q-1\}$ and $k \geq 2$. These equivalences can be denoted as $W_{G_q}^{(i)} \equiv \tilde{W}^{\otimes k}$ and $W_{G_q}^{(i)} \equiv W \otimes \tilde{W}^{\otimes k-1}$, where \equiv means that both channels are stochastically degraded with respect to each other.

Now, we introduce the concept of partial distance:

Definition 6. For a kernel $g: \mathcal{X}^q \rightarrow \mathcal{X}^q$, the partial distance D_i is given as

$$D_i = \min_{v_{i+1}^{q-1}, w_{i+1}^{q-1}} d\left(g\left(s_0^{i-1}, x, v_{i+1}^{q-1}\right), g\left(s_0^{i-1}, x', w_{i+1}^{q-1}\right)\right) \quad (25)$$

where $a, b \in \mathcal{X}^q$, $d(a, b)$ is the Hamming distance between a and b .

Thus, we can define the RS kernel as $G_q = [g_0^T, \dots, g_{q-1}^T]^T$. Since it is generated by a Reed-Solomon code, which is a maximum distance separable code, the partial distance of RS kernel is $D_i = i+1$. Then, we can rewrite $W_{G_q}^{(i)}$ using equation (19) and (20) as follows:

$$W_{G_q}^{(i)} = \frac{1}{q^{q-1-i}} \sum_{c_0^{q-1} \in \Lambda(s_0^i)} \prod_{k=0}^{q-1} W(y_k | c_k) \quad (26)$$

where $\Lambda(s_0^i) \subset \{0, \dots, q-1\}^{q-1}$ and c_0^{q-1} satisfying

$$c_0^{q-1} = \sum_{j=0}^{i-1} s_j g_j + s_i g_i + \sum_{j=i+1}^{q-1} v_j g_j \quad (27)$$

for some $v_{i+1}^{q-1} \in \{0, \dots, q-1\}^{q-1-i}$. Let $g_\delta = \sum_{j=i+1}^{q-1} \delta_j g_j$ be a codeword and satisfying

$$\min_{v_{i+1}^{q-1}, w_{i+1}^{q-1}} d\left(g\left(s_0^{i-1}, x, v_{i+1}^{q-1}\right), g\left(s_0^{i-1}, x', w_{i+1}^{q-1}\right)\right) = D_i \quad (28)$$

Due to the linearity of $\langle g_{i+1}, \dots, g_{q-1} \rangle$, it's equivalent to say that $c_0^{q-1} \in \Lambda(s_0^i)$ if and only if

$$c_0^{q-1} = \sum_{j=0}^{i-1} s_j g_j + s_i (g_i + g_\delta) + \sum_{j=i+1}^{q-1} v_j g_j \quad (29)$$

Therefore, we can define $G'_q = [g_0^T, \dots, g_i^T, \dots, g_{q-1}^T]^T$, where $g'_i = g_i + g_\delta$. At this point, the partial distance of g'_i in

G'_q is equal to D_i . Furthermore, the channels $W_{G'_q}^{(i)}$ and $W_{G_q}^{(i)}$ are equivalent based on (27) and (29).

Now, consider a channel $W_{g,q}^{(i)}$ where a genie provides extra information (s_{i+1}^{q-1}) to the decoder of $W_{G'_q}^{(i)}$, then the $W_{G'_q}^{(i)}$ can be seen as a degradation of the channel $W_{g,q}^{(i)}$. The transition probabilities of this $W_{g,q}^{(i)}$ are defined as

$$W_{g,q}^{(i)}\left(y_0^{q-1}, s_0^{i-1}, s_{i+1}^{q-1} | s_i\right) = \frac{1}{q^{q-1}} \prod_{j=0}^{q-1} W\left(y_j | \left(s_0^{q-1} G'_q\right)_j\right) \quad (30)$$

Since the matrix G'_q is invertible, referring to the definition of D_i , it follows that there exists a set $J = \{j | j \in \{0, 1, \dots, q-1\}\}$ and $|J| = D_i$ such that the genie-aided channel $W_{g,q}^{(i)}$ can be expressed as below:

$$\begin{aligned} & W_{g,q}^{(i)}\left(y_0^{q-1}, s_0^{i-1}, s_{i+1}^{q-1} | s_i\right) \\ &= \left(\frac{1}{q^{|J|}} \prod_{j \in J} W\left(y_j | s_i G'_{q(i,j)} + (s G'_q)_j - s_i G'_{q(i,j)}\right) \right) \\ & \cdot \left(\frac{1}{q^{q-1-|J|-1}} \prod_{j \in J^c} W\left(y_j | (s G'_q)_j\right) \right) \end{aligned} \quad (31)$$

It satisfies that the second term on the right-hand side of the above equality is independent of the input s_i . Thus, the $W_{g,q}^{(i)}$ is equivalent to either $\tilde{W}^{\otimes D_i}$ or $W \otimes \tilde{W}^{\otimes D_i-1}$ and $Z\left(\tilde{W}^{\otimes D_i}\right) = Z\left(W \otimes \tilde{W}^{\otimes D_i-1}\right) = Z(W)^{D_i}$. As the partial distance of RS kernel is $D_i = i+1$ and $0 < Z(W) < 1$, the ordering of Bhattacharyya parameter is $Z(W_{g,q}^{(i+1)}) \preceq Z(W_{g,q}^{(i)})$. Note that $W_{G'_q}^{(i)}$ can be seen as a degradation of channel $W_{g,q}^{(i)}$ which can be expressed as

$$Z(W_{G'_q}^{(i)}) = Z(W_{g,q}^{(i)}) + \Delta(W, i) \quad (32)$$

where $\Delta(W, i)$ is the incremental function of the Bhattacharyya parameter after channel degradation, which is related to the input channel W and the sub-channel index i . Note that in the single-layer RS kernel, the degradation decreases with increasing channel index i . Therefore, it's easy to express that the relationship for the channel reliability of the sub-channels in RS kernel as $W_{G_q}^{(i)} \preceq W_{G_q}^{(i+1)}$.

B. Partial Orders of RS Polar Codes

Definition 7. (Addition Operator): Denote $(i_{m-1}, \dots, i_1, i_0)$ as the q -ary representation of the index i in (13). Given $k \in \{0, 1, \dots, m-1\}$, the Addition Operator at position k maps i into $A^{(k)}(i) \in \{0, 1, \dots, N-1\}$. If $i_k = q-1$ then $A^{(k)}(i) = i$. Otherwise, the q -ary representation of $A^{(k)}(i)$ is defined as

$$\left(A^{(k)}(i)\right)_\ell = \begin{cases} i_\ell + 1, & \ell = k, \\ i_\ell, & \ell \neq k. \end{cases} \quad (33)$$

Proposition 1. Let W be a q -ary memoryless output symmetric channel W and the synthetic sub-channel $W_N^{(i)}$ is obtained

from W by applying (12). Then, for any $i \in \{0, 1, \dots, N-1\}$, $W_N^{(i)} \preceq W_N^{(A^{(k)}(i))}$.

Proof: Let i be the index of synthetic sub-channel $W_N^{(i)}$, and let the q -ary representation of i be $(i_{m-1}, \dots, i_1, i_0)$, where $i \in \{0, 1, \dots, N-1\}$ and $i_k \in \{0, 1, \dots, q-1\}$. The $A^{(k)}(i)$ operation is the selection of different split channels in a single-layer RS kernel. As shown in the previous subsection, for the same $q \times q$ RS kernel G_q , the reliability representation of sub-channels can be express as $W_{G_q}^{(i_k)} \preceq W_{G_q}^{(i_{k+1})}$. This means that compared to sub-channel i , the reliability of the input channel of sub-channel $A^{(k)}(i)$ increases from the k -th layer kernel, while the subsequent polarization process remains unchanged, so the final channel reliability is higher. Thus, for any $i \in \{0, 1, \dots, N-1\}$, $W_N^{(i)} \preceq W_N^{(A^{(k)}(i))}$ which concludes the proof. ■

Example 1. Consider the RS polar code over $\mathcal{GF}(4)$ with $m = 3$ and index $i = 25$, its q -ary representation is $(1, 2, 1)$. Then, after $A^{(1)}(25)$, we get the $i = 29$ with $(1, 3, 1)$. Applying the Proposition 1, we conclude $W_{64}^{(25)} \preceq W_{64}^{(29)}$.

Definition 8. (Left-Swap Operator): Denote $(i_{m-1}, \dots, i_1, i_0)$ as the q -ary representation of the index i in (13). Given $k_1, k_2 \in \{0, 1, \dots, m-1\}$ and $k_1 < k_2$, the Left-Swap operator at position k_1 and k_2 maps i into $L^{(k_1, k_2)}(i) \in \{0, 1, \dots, N-1\}$. If $i_{k_1} \leq i_{k_2}$ then $L^{(k_1, k_2)}(i) = i$. Otherwise, the q -ary representation of $L^{(k_1, k_2)}(i)$ is defined as

$$\left(L^{(k_1, k_2)}(i) \right)_\ell = \begin{cases} i_{k_2}, & \ell = k_1, \\ i_{k_1}, & \ell = k_2. \\ i_\ell, & \ell \notin \{k_1, k_2\}. \end{cases} \quad (34)$$

Proposition 2. Let W be a q -ary memoryless output symmetric channel W and the synthetic sub-channels $W_N^{(i)}$ are obtained from W by applying (12). Then, for any $i \in \{0, 1, \dots, N-1\}$, $W_N^{(i)} \preceq W_N^{(L^{(k_1, k_2)}(i))}$.

Proof: Let W be a q -ary memoryless output symmetric channel. First consider the case $k_2 = k_1 + 1$, which can be seen as two adjacent polarization operations based on the RS kernel G_q i.e $G_q^{\otimes 2}$. Denote $N_2 = q^2$, the transition probability of suchannel $W_{N_2}^{(i)}$ is shown as

$$W_{N_2}^{(i)} \left(y_0^{N_2-1}, s_0^{i-1} \mid s_i \right) = \frac{1}{q^{N_2-1}} \sum_{s_{i+1}^{N_2-1}} W_{N_2}^{(i)} \left(y_0^{N_2-1} \mid s_0^{N_2-1} \right) \quad (35)$$

Consider the channel $W_{g, N_2}^{(i)}$ as the genie-added channel of $W_{N_2}^{(i)}$ and its transition probability is defined as

$$\begin{aligned} & W_{g, N_2}^{(i)} \left(y_0^{N_2-1}, s_0^{i-1}, s_{i+1}^{N_2-1} \mid s_i \right) \\ &= \frac{1}{q^{N_2-1}} \prod_{j=0}^{N_2-1} W \left(y_j \mid \left(s_0^{N_2-1} G_q^{\otimes 2} \right)_j \right) \end{aligned} \quad (36)$$

According to the proof in the previous subsection, $W_{g, N_2}^{(i)}$ is equivalent to $(\tilde{W}^{\otimes k_1})^{\otimes k_2}$ that is

$$Z(W_{g, N_2}^{(i)}) = Z(W_{g, N_2}^{(L^{(k_1, k_2)}(i))}) = Z(W)^{(i_{k_1+1}) * (i_{k_2+1})} \quad (37)$$

Here, we can assume that in the ideal case, $s_{L^{(k_1, k_2)}(i)}$ and s_i pass through channels $W_{g, q}^{(i_{k_1})}$ and $W_{g, q}^{(i_{k_2})}$ in different orders with the similar degradation pattern, but more outputs are omitted in $W_{N_2}^{(i)}$ compared to $W_{N_2}^{(L^{(k_1, k_2)}(i))}$. Therefore, $W_{N_2}^{(i)}$ is stochastically degraded with respect to $W_{N_2}^{(L^{(k_1, k_2)}(i))}$ i.e.

$$\begin{aligned} W_{N_2}^{(L^{(k_1, k_2)}(i))} &\equiv s_i \rightarrow \left(y_0^{N_2-1}, s_0^{L^{(k_1, k_2)}(i)-1} \right) \\ &\succeq s_i \rightarrow \left(y_0^{N_2-1}, s_0^{i-1} \right) \\ &\equiv W_{N_2}^{(i)} \end{aligned} \quad (38)$$

On the basis of the adjacent RS kernel, the reliability of the sub-channel can be passed to the left in the q -ary representation index through the expression (38). Thus, when $k_2 - k_1 > 1$, $W_{N_2}^{(L^{(k_1, k_2)}(i))} \succeq W_{N_2}^{(i)}$ also holds which concludes the proof. ■

Example 2. Consider the RS polar code based $\mathcal{GF}(4)$ with $m = 3$ and index $i = 27$, its q -ary representation is $(1, 2, 3)$. Then, after $L^{(0, 2)}(27)$, we get the index $i = 57$ with $(3, 2, 1)$. Applying the Proposition 2, we conclude $W_{64}^{(27)} \preceq W_{64}^{(57)}$.

Proposition 3. (Quasi-Nested) The reliability orders of sub-channels determined for an RS polar code of length N by partial orders remain unchanged in code length of qN .

Proof: Denote $(i_{m-1}, \dots, i_1, i_0)$ as the q -ary representation of RS kernel polar code in length N . Then, in the length qN , $(0, i_{m-1}, \dots, i_1, i_0)$ also follows the above two partial orders. ■

C. Partial Distance-based Polarization Weight Construction Method

The concept of Polarization Weight (PW) was initially introduced in [26] to construct polar codes with Arikan kernel. In the previous subsection, we demonstrated that the reliability of a sub-channel is closely linked to the partial distance of its corresponding index in the single-layer RS kernel. Moreover, holding other conditions constant, the reliability of the subchannel increases with the number of layers. As a result, we propose a Partial Distance-based Polarization Weight (PDPW) construction method in this section, which has low computational complexity.

Our investigation revealed that, in RS polar codes, the reliability of a sub-channel with an index i $(i_{m-1}, \dots, i_1, i_0)$, where $i_k \in \{0, 1, \dots, q-1\}$, can be seen as being affected by two factors. We refer to these factors as the intra-layer polarization effect associated with i_k and the inter-layer polarization effect related to k . Since the reliability of sub-channel with genie-added $W_{g, N}^{(i)}$ can be represented by $Z(W)^{\prod_{k=0}^{m-1} D_{i_k}}$ with $0 < Z(W) < 1$, we represent the reliability of sub-channel with genie-added by

$$w_{g, N}(i) \mapsto \prod_{k=0}^{m-1} D_{i_k} \quad (39)$$

where the higher the value of $w_{g,N}(i)$ is, the greater its reliability. However, since $W_{g,N}(i)$ is an ideal situation, we factor in the two influencing factors mentioned earlier to adjust its value. Using the concept of polarization weight, we represent the reliability of a sub-channel $W_N^{(i)}$ by

$$w(i) \mapsto \prod_{k=0}^{m-1} D_{i_k}^{\zeta(i_k)\beta^k} \quad (40)$$

where $\zeta(i_k)$ and β^k denote the correction factors for the intra-layer polarization effect and inter-layer polarization effect, respectively. To simplify the computation, we introduce logarithms and derive the final form of the PDPW construction method as shown in Definition 9.

Definition 9. (PDPW): For a $N = q^m$ polar code with RS kernel, denote $(i_{m-1}, \dots, i_1, i_0)$ as the q -ary representation of the index i in (13) and D_{i_k} as the the partial distance of the index i_k in a single-layer kernel. Then, the Partial Distance-based Polarization Weight $w(i)$ is defined as

$$f^{\text{PDPW}} : w(i) \mapsto \sum_{k=0}^{m-1} \zeta(i_k)\beta^k \log_2 D_{i_k} \quad (41)$$

where β^k and $\zeta(i_k)$ are the correction factors for inter-layer polarization effect and intra-layer polarization effect, respectively. These numbers require careful selection, backed by comprehensive experimentation and justification.

As discussed earlier, the sub-channel $W_{G_q}^{(i)}$ in the single-layer RS kernel can be interpreted as the degradation of the genie-added channel $W_{g,q}^{(i)}$. Consequently, $\zeta(i)$ can be viewed as the proportion of the sub-channel's reliability relative to the genie-added channel in a single RS kernel. Through the simulation tests, we observed that under certain channel conditions, $\zeta(i)$ can be approximated by mutual information as below:

$$\zeta(i) = \frac{I(W_{G_q}^{(i)})}{I(W_{g,q}^{(i)})} \quad (42)$$

Referring to [28], one can use Monte-Carlo simulations to approximate the mutual information of the corresponding channel by calculating the entropy of the symbol probabilities in the single-layer RS kernel and averaging them over sufficiently large number of channel output instances. Denote $H(S_i)$ as the entropy function of S_i , $Pr_i(\eta) = W_{G_q}^{(i)}(Y_0^{q-1}, S_0^{i-1} | S_i = \eta)$ and $Pr'_i(\eta) = W_{g,q}^{(i)}(Y_0^{q-1}, S_0^{i-1}, S_{i+1}^{q-1} | S_i = \eta)$, where S_i is a random variable corresponding to the i -th input symbol of the single RS kernel and $\eta \in \mathcal{GF}(q)$. Then the corresponding mutual information functions can be calculated as follows:

$$\begin{aligned} I(W_{G_q}^{(i)}) &= H(S_i) - H(Y_0^{q-1}, S_0^{i-1} | S_i) \\ &\approx \frac{1}{T} \sum_{z=0}^T \hat{I}_z(W_{G_q}^{(i)}) \end{aligned} \quad (43)$$

where

$$\hat{I}_z(W_{G_q}^{(i)}) = H(S_i) + \sum_{\eta \in \mathcal{GF}(q)} Pr_i(\eta) \log_2(Pr_i(\eta)) \quad (44)$$

Since $W_{g,q}^{(i)}$ is the channel with genie-added information, we assume that the Bhattacharyya parameter of $W_{g,q}^{(i)}$ in the single-layer RS kernel reaches its average error probability bound i.e.

$$P_e(W_{g,q}^{(i)}) \approx (q-1)Z(W_{g,q}^{(i)}) = (q-1)Z(W)^{D_i} \quad (45)$$

We can then approximate the value of $Pr'_i(\eta)$ by $W_{G_q}^{(q-1)} = W_{g,q}^{(q-1)}$. Next, calculating $I(W_{g,q}^{(i)})$ by using the above mutual information approximation functions and finally obtaining the $\zeta(i)$ corresponding to the sub-channel within a single-layer RS kernel. Note that the coefficient $\zeta(0)$ can be directly assigned a value of zero as it does not make a contribution to the polynomial. Similarly, the coefficient $\zeta(q-1)$ can be directly set to one as the entire assumption is based on the premise of $W_{G_q}^{(q-1)} = W_{g,q}^{(q-1)}$.

For the coefficient β , as k is the non-negative, $\beta^k > 0$ which follows the Addition partial order. To achieve the Left-Swap partial order, β should satisfy $\beta^k < \beta^{k+j}$ for any non-negative integer k and positive integer j , which implies that $\beta > 1$. Once the coefficient $\zeta(i_k) \log_2 D_{i_k}$ is obtained, the value of β can be approximated using a polynomial equation solver, as described in [26].

Example 3. Taking RS kernel G_4 as an example. The coefficient $\zeta(i)$ of G_4 at different signal-to-noise ratios (SNR) over additive white Gaussian noise (AWGN) channels are shown in Table I. Here we choose the $\zeta(i)$ values at $E_b/N_0 = -1.8\text{dB}$ as in the Monte-Carlo method, which have the best pre-test performance.

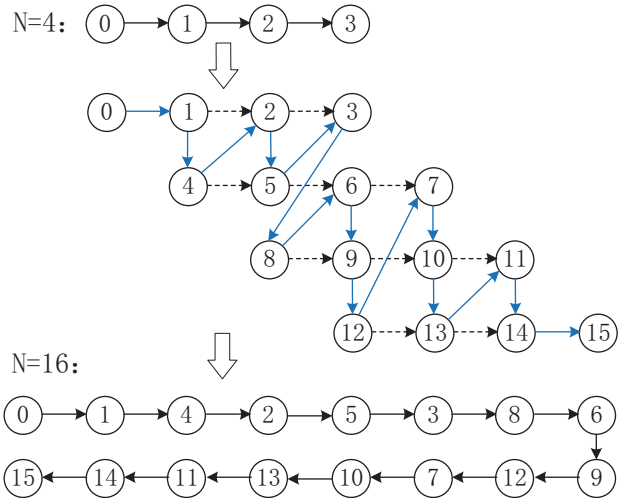


Fig. 3. Polarization weights of sub-channels with block length $N=256$

When the block length increases, the uncertainty relation among them is calculated according to the actual situation, and the interval of β is approximated. Fig.3. illustrates how the range of β evolves as the block length increases from $N=4$ to $N=16$ over AWGN channels. The uncertainty relations

including (3,8), (7,12), (10,13) etc. are calculated on the basis of $\beta > 1$ as follows:

$$\begin{aligned} 7 > 12 &\iff \beta < 1.55 \\ 13 > 10 &\iff \beta > 1.12 \\ 8 > 3 &\iff \beta > 1.437 \end{aligned}$$

Thus, we obtain an approximate range (1.437, 1.55) for β . Then, by increasing the block size, a more accurate range of β can be calculated.

Let $\beta = 1.512$ and the block length is set to $N = 256$. Then, the weight of the sub-channel with index 99, i.e., (1, 2, 0, 3) can be computed as

$$\begin{aligned} w(99) &= \zeta(1)\beta^3 \log_2 2 + \zeta(2)\beta^2 \log_2 3 + 0 + \zeta(3)\beta^0 \log_2 4 \\ &= 7.648 \end{aligned}$$

Similarly, we can construct the polarization weights of the sub-channels of the overall codeword, as shown in Fig.4.

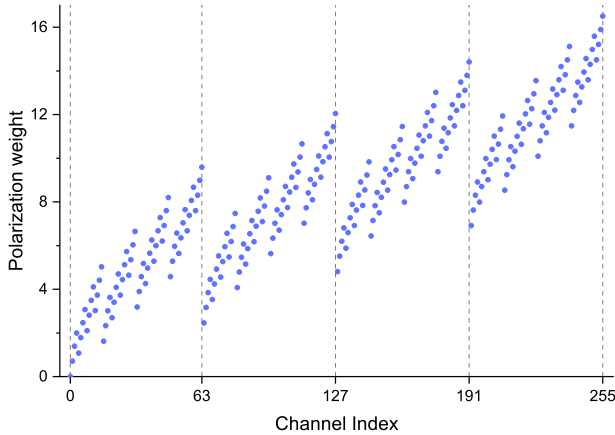


Fig. 4. Polarization weights of sub-channels over G_4 with block length $N = 256$

Finally, we analyze the complexity of the proposed construction method. Denote Ω as the complexity of a single evaluation of (12). The complexity of the approximate functions $\zeta(i)$ is $\mathcal{O}(Tq\Omega)$ and the PDPW construction complexity is $\mathcal{O}(N)$. In comparison, the complexity of the Monte-Carlo method can be expressed as $\mathcal{O}(TN \log_q(N)\Omega)$. Compared to classical Monte-Carlo simulation, the proposed PDPW method requires only one approximation of the mutual information of sub-channels for a single-layer RS kernel, thus greatly reducing the construction complexity.

IV. MINIMUM POLARIZATION WEIGHT PUNCTURING SCHEME

Puncturing is an efficient rate-matching technique that is commonly used in 5G communication standards for low-rate polar codes [12]. Fixed information set is an essential part of incremental redundancy hybrid automatic repeat request (IR-HARQ) in 3GPP NR. Referring to the PDPW construction method in the previous section, we propose Minimum Polarization weight Puncturing (MPWP) algorithm for fixed information set which is shown as follows:

Denote the N symbols length polar codes with RS kernel in bits as $N_b = tq^m$. According to the transmission requirements, the actual number of transmitted bits is M_b , where $M_b < N_b$.

- Based on the polarization weights of the subchannels, the fixed information set can be selected as \mathcal{I} . Then, from the set \mathcal{I}^c , $l + 1$ subchannels with the smallest weights are selected to determine the puncturing symbols vector $\mathcal{R}_p = (r_0, r_1, \dots, r_{l-1})$, where $l = \lceil (N_b - M_b)/t \rceil$ and $w(r_0) < w(r_1) < \dots < w(r_{l-1})$.
- On the encoder side, do not transmit the first $l-1$ symbols of \mathcal{R}_p that is freezing them in input symbols s_0^{N-1} . Note that for index r_{l-1} , special judgments are required: Denote $\sigma = (N_b - M_b) \bmod t$. If $\sigma > 0$, disable the last σ bits of q -ary representation of index r_{l-1} . Otherwise, disable the whole symbol r_{l-1} .
- On the decoding side, the decoding architecture is not changed. Since the symbols and bits represented in \mathcal{R}_p are not actually transmitted, their corresponding LLRs are set to 0.

V. SIMULATION RESULTS

In this section, we present the simulation results for the proposed construction method and rate-matching algorithm. For the following simulations, the RS polar codes are over $\mathcal{GF}(4)$ and exploited the CA-SCL decoding algorithm with CRC=8 bits and list size $L=2$. All codewords are modulated using the binary phase-shift keying (BPSK) and transmitted over additive white Gaussian noise (AWGN) channels.

In the first trial, we evaluate the performance of the proposed construction method at code rates $R=1/3$, $R=1/2$, and $R=2/3$. Fig.5 and Fig.6 illustrate the performance of the proposed PDPW construction method and the Monte-Carlo method with symbol lengths of $N = 1024$ and $N = 256$, respectively. As expected, the performance of the two construction methods is essentially the same for the two block lengths and three code rates. Fig.6 also includes the performance of 3GPP NR polar codes over Arikan kernel with a bit length of $N_b = 512$ for comparison. Overall, the performance of the proposed PDPW construction method over $\mathcal{GF}(4)$ RS kernel is better than 3GPP polar codes over Arikan kernel. Specifically when $\text{BLER}=10^{-3}$, the proposed method yields nearly 0.23db and 0.27db gain over 3GPP NR polar codes for rates of $R=1/3$ and $R=1/2$ respectively.

Then, we will mainly compare the rate-matching performance for fixed information set. In the following simulations, the information set is optimized by the mother codes. Fig.7. shows the performance of the proposed algorithm and the smallest index puncturing (SIP) algorithm [22] over $\mathcal{GF}(4)$ with mother code length $N = 1024$ and actual block length $M = 800$. In this trial, our proposed algorithm performs the same as SIP at a low code rate but has a larger gain at a higher code rate. This is because our algorithm retains more highly reliable sub-channels when the code rate is increased.

Furthermore, Fig.8. illustrates the puncturing performance of the proposed method over $\mathcal{GF}(4)$ RS kernel and the 3GPP NR polar codes over Arikan kernel. Note the 3GPP NR polar codes are constructed utilizing the 3GPP channel reliability

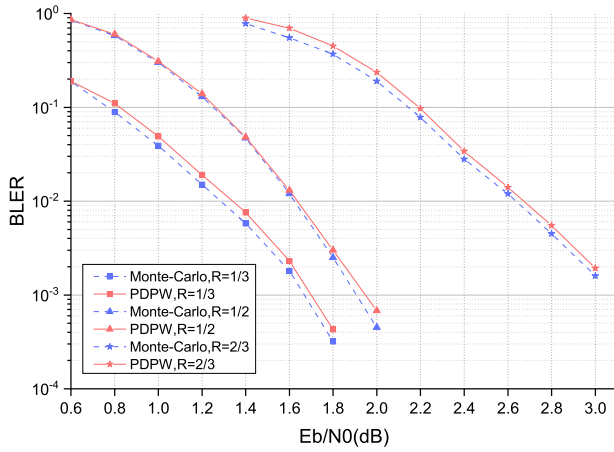


Fig. 5. Performance of RS polar codes with block length $N = 1024$

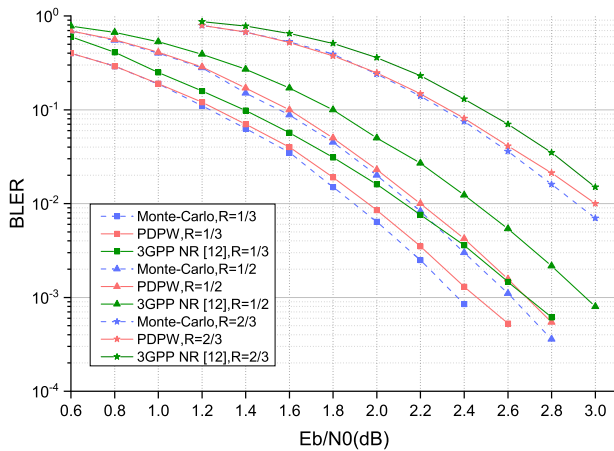


Fig. 6. Performance of RS polar codes and 3GPP NR polar codes with block length $N_b = 512$

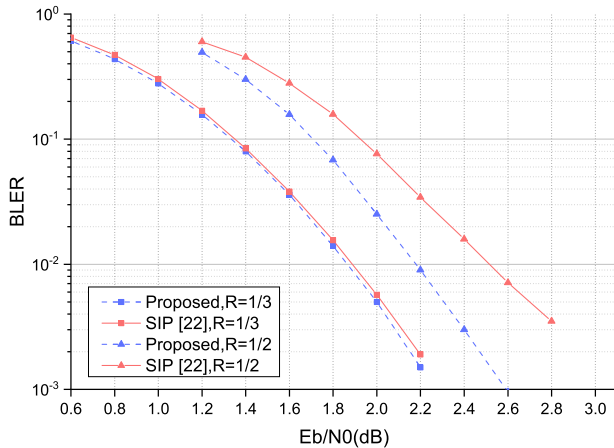


Fig. 7. Rate-matching performance of RS polar codes with block length $N = 1024$ and $M = 800$

table and applied pre-frozen set regarded as an optimization of the puncturing method in 3GPP NR [12]. This simulation tests the SNR required to achieve $\text{BLER}=10^{-3}$ for two codewords at different lengths. The length of the mother code $N_b = 512$, the overall code rate is $R = 1/3$. Results indicate that for most

lengths greater than 340, the proposed puncturing algorithm for RS polar codes achieves a gain of approximately 0.2dB compared to the 3GPP NR polar codes.

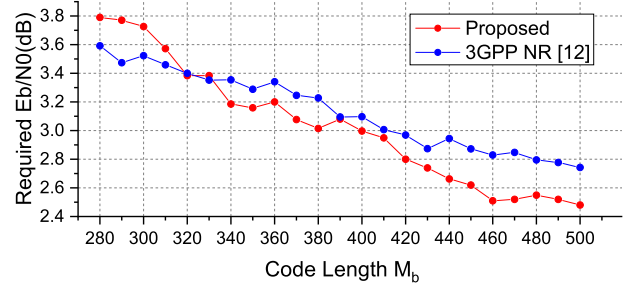


Fig. 8. Schematic diagram of the required E_b/N_0 for different codes to manage a performance of $\text{BLER}=10^{-3}$

VI. CONCLUSION

In this work, we investigate the partial orders of polar codes with RS kernel and propose a PDPW construction method based on these partial orders, as well as an MPWP puncturing algorithm. The performance of the proposed construction method is nearly identical to that of the Monte Carlo method, and the proposed puncturing algorithm outperforms the current SIP algorithm. Based on the proposed construction scheme, both the standard codeword performance and rate-matching performance of RS polar codes are superior to the 3GPP NR polar codes. Therefore, RS polar codes can be considered an important candidate for channel coding in the next generation of communication systems.

For multi-kernel polar codes, due to the increasing complexity of the kernel, the decoding algorithm becomes a critical area for future research. Specifically, developing a lower-complexity approach for processing soft information in different multi-kernels during the decoding algorithm is of utmost importance for improving the practicality and effectiveness of these codes.

REFERENCES

- [1] E. Arıkan, "Channel Polarization: A Method for Constructing Capacity-Achieving Codes for Symmetric Binary-Input Memoryless Channels," *IEEE Trans. Inf. Theory*, vol. 55, no. 7, pp. 3051-3073, July. 2009.
- [2] I. Tal and A. Vardy, "List Decoding of Polar Codes," *IEEE Trans. Inf. Theory*, vol. 61, no. 5, pp. 2213-2226, May. 2015.
- [3] S. A. Hashemi, C. Condo, and W. J. Gross, "A fast polar code list decoder architecture based on sphere decoding," *IEEE Trans. Circuits Syst. I, Reg. Papers*, vol. 63, no. 12, pp. 2368-2380, Dec. 2016.
- [4] M. Hanif, M. H. Ardakani, and M. Ardakani, "Fast list decoding of polar codes: Decoders for additional nodes," in Proc. *IEEE Wireless Commun. Netw. Conf. Workshops (WCNCW)*, Apr. 2018, pp. 37-42.
- [5] K. Niu and K. Chen, "Stack decoding of polar codes," *Electronics Letters*, vol. 48, no. 12, pp. 695-696, 2012.
- [6] L. Xiang, S. Zhong, R. G. Maunder and L. Hanzo, "Reduced-Complexity Low-Latency Logarithmic Successive Cancellation Stack Polar Decoding for 5G New Radio and Its Software Implementation," in *IEEE Transactions on Vehicular Technology*, vol. 69, no. 11, pp. 12449-12458, Nov. 2020.
- [7] H. Zhou, W. Song, W. J. Gross, Z. Zhang, X. You and C. Zhang, "An Efficient Software Stack Sphere Decoder for Polar Codes," in *IEEE Transactions on Vehicular Technology*, vol. 69, no. 2, pp. 1257-1266, Feb. 2020.
- [8] I. Tal and A. Vardy, "How to construct polar codes," *IEEE Trans. Inf. Theory*, vol. 59, no. 10, pp. 6562-6582, Oct. 2013.

- [9] P. Trifonov, "Efficient design and decoding of polar codes," *IEEE IEEE Trans. Commun.*, vol. 60, no. 11, pp. 3221–3227, Nov. 2012.
- [10] K. Niu, K. Chen, and J. Lin, "Beyond turbo codes: Rate-compatible punctured polar codes," in *Proc. IEEE ICC*, pp. 3423–3427, June. 2013.
- [11] J. Zhao, W. Zhang, and Y. Liu, "A novel puncturing scheme of low rate polar codes based on fixed information set," *IEEE Commun. Lett.*, vol. 25, no. 7, pp. 2104–2108, Jul. 2021.
- [12] *NR Multiplexing Channel Coding (Release 15)*, document TSG RAN TS38.212 V15.5.0, 3GPP, Mar. 2019.
- [13] V. Bioglio, F. Gabry, I. Land and J. -C. Belfiore, "Multi-Kernel Polar Codes: Concept and Design Principles," in *IEEE Transactions on Communications*, vol. 68, no. 9, pp. 5350-5362, Sept. 2020
- [14] C. Xia, C. -Y. Tsui and Y. Fan, "Construction of Multi-Kernel Polar Codes With Kernel Substitution," in *IEEE Wireless Communications Letters*, vol. 9, no. 11, pp. 1879-1883, Nov. 2020
- [15] S. B. Korada, E. Şaşıoğlu and R. Urbanke, "Polar Codes: Characterization of Exponent, Bounds, and Constructions," in *IEEE Transactions on Information Theory*, vol. 56, no. 12, pp. 6253-6264, Dec. 2010
- [16] R. Mori and T. Tanaka, "Channel polarization on q-ary discrete memoryless channels by arbitrary kernels," in *Proc. IEEE ISIT 2010*, Austin, 2010.
- [17] P. Trifonov and V. Miloslavskaya, "Polar Subcodes," in *IEEE Journal on Selected Areas in Communications*, vol. 34, no. 2, pp. 254-266, Feb. 2016.
- [18] F. Abbasi, H. Mahdaviifar and E. Viterbo, "Hybrid Non-Binary Repeated Polar Codes," in *IEEE Transactions on Wireless Communications*, vol. 21, no. 9, pp. 7582-7594, Sept. 2022.
- [19] R. Mori and T. Tanaka, "Non-binary polar codes using Reed-Solomon codes and algebraic geometry codes," in *Proc. IEEE Inf. Theory Workshop*, Dublin, OH, USA, Aug./Sep. pp. 1–5. 2010.
- [20] N. Cheng, R. Zhang, Y. Ge, W. Shi, Q. Zhang, and X. Shen, "Encoder and list decoder of Reed-Solomon kernel based polar codes," in *Proc. IEEE WCSP 2016*, Yangzhou, China. pp. 1-6, 2016.
- [21] P. Trifonov, "Binary successive cancellation decoding of polar codes with Reed-Solomon kernel," in *Proc. IEEE ISIT 2014*, Honolulu, HI, USA, 2010.
- [22] R. Zhang, H. Saber, Y. Ge and W. Shi, "Rate-matching and Piecewise Sequence Adaptation for Polar Codes with Reed-Solomon Kernels," in *018 10th International Conference on Wireless Communications and Signal Processing (WCSP)*, pp. 1–6, Dec. 2018.
- [23] C. Schürch, "A partial order for the synthesized channels of a polar code," in *2016 IEEE International Symposium on Information Theory (ISIT)*, pp. 220-224, 2016.
- [24] M. Bardet, V. Dragoi, A. Otmani and J. -P. Tillich, "Algebraic properties of polar codes from a new polynomial formalism," *2016 IEEE International Symposium on Information Theory (ISIT)*, Barcelona, Spain, 2016.
- [25] W. Wu and P. H. Siegel, "Generalized Partial Orders for Polar Code Bit-Channels," in *IEEE Transactions on Information Theory*, vol. 65, no. 11, pp. 7114-7130, Nov. 2019.
- [26] G. He, J. Belfiore, I. Land, G. Yang, X. Liu, Y. Chen, R. Li, J. Wang, Y. Ge, R. Zhang, and W. Tong, "Beta-expansion: A theoretical framework for fast and recursive construction of polar codes," in *Proc. IEEE Global Commun. Conf.(GLOBECOM)*, pp. 1–6, Dec. 2017.
- [27] M. Mondelli, S. H. Hassani and R. Urbanke, "Construction of polar codes with sublinear complexity," *2017 IEEE International Symposium on Information Theory (ISIT)*, Aachen, Germany, 2017.
- [28] J. Kliewer, S. X. Ng, and L. Hanzo, "Efficient computation of EXIT functions for nonbinary iterative decoding," *IEEE Trans. Commun.*, vol. 54, no. 12, pp. 2133–2136, Dec. 2006.